Synthesis of ZnO films with a special texture and enhanced field emission properties*

Wang Xiao-Ping(王小平)[a)†], Wang Zi(王 子)[b)], Wang Li-Jun(王丽军)[a)], and Mei Cui-Yu(梅翠玉)[a)]

[a)] College of Science, University of Shanghai for Science and Technology, Shanghai 200093, China
[b)] School of Transportation Engineering, Tongji University, Shanghai 200092, China

(Received 18 April 2011; revised manuscript received 30 May 2011)

ZnO films with special textures are fabricated on Mo-coated Al_2O_3 ceramic substrates by the catalyst-free electron beam evaporation method, and the as-deposited films are treated by hydrogen plasma. It is found that the surface morphologies of the films are changed significantly after hydrogen plasma treatment and that the films consist of vertically standing and intersecting nanosheets. A lower turn-on field of 1.2 V/μm and an enhanced current density ∼0.11 mA/cm^2 at 2.47 V/μm are achieved. The low threshold field and the high emission current density are attributed primarily to the unique shape and smaller resistivity of the ZnO nanosheet films.

Keywords: nano-ZnO thin films, hydrogen plasma treatment, field electron emission, microwave plasma chemical vapour deposition

PACS: 52.77.–j, 79.60.Jv, 79.70.+q **DOI:** 10.1088/1674-1056/20/10/105203

1. Introduction

ZnO material, an intrinsical n-type semiconductor with a wide direct band gap of ∼3.37 eV and large exciton binding energy of ∼60 meV, has been extensively studied in recent years due to its potential applications in optical and electronic devices.[1−19] At present, it has been widely used in piezoelectric transducers, varistors, gas sensors, catalysts and transparent conducting films.[14−16] The growth characteristics of a nanometer ZnO array on n-type silicon substrate was systematically explored by Lee *et al.*[6] They also examined the field electron (FE) emission properties of ZnO-nanowires prepared by using cobalt as a catalyst. To obtain a current density of 0.1 μA/cm^2, an external electric field of 6.0 V/μm is required, and to obtain a current density of 1.0 μA/cm^2, a higher field (∼11 V/μm) is needed. Xu and Sun[7] reported investigations on the FE properties of ZnO nanowires and found that the current density of the nanowire was only 0.1 μA/cm^2 under an applied electric field of 1.9 V/μm.

In the present paper, a series of nano-structured ZnO films (NZFs) is fabricated using catalyst-free electron beam evaporation techniques and these as-grown films are etched by hydrogen plasma. The surface morphologies, microstructures and FE characteristics are studied for the NZFs. It is found that the surface morphologies each undergo a remarkable change for those NZFs treated by the hydrogen plasma etching, which consists of vertically standing and intersecting nanosheets. A current density of ∼0.11 mA/cm^2 at 2.47 V/μm and a threshold electric field of 1.2 V/μm are obtained. The lower turn-on field and the high emission current density are interpreted.

2. Experiment and discussion

2.1. Fabrication of ZnO thin films

The electron beam evapouration deposition (EBVD) system was used to deposit NZFs on Mo film-coated Al_2O_3 ceramic substrates, with high purity (99.99%) ZnO used as a deposition target. The specific parameters used for the EBVD process are listed in Table 1, resulting in a 1000-Å (1 Å = 0.1 nm) thick ZnO film (controlled by a film thickness monitor).

Then the ZnO film was hydrogen plasma treated by a microwave plasma chemical vapour deposition (MPCVD) technique. The specific parameters used for the MPCVD process are listed in Table 2.

*Project supported by the Science Foundation of Shanghai Human Resources and Social Security Bureau, China (Grant No. 2009023).

†Corresponding author. E-mail: wxpchina64@yahoo.com.cn

© 2011 Chinese Physical Society and IOP Publishing Ltd

Table 1. Parameters employed for the EBVD process.

EBVD process parameters	Values
Beam current/mA	20
Vacuum/kPa	2.0×10^{-3}
Substrate temperature/°C	527
Voltage/kV	6
Vapour time/min	40
Filament current/mA	0.6
Oxygen gas flow/sccm	4

Table 2. Parameters employed for the MPCVD process.

MPCVD process parameters	Values
Hydrogen gas flows/sccm	100
Total gas pressure/kPa	5.5
Substrate temperature/°C	750
Plasma processing time/min	20
Microwave power/W	1300

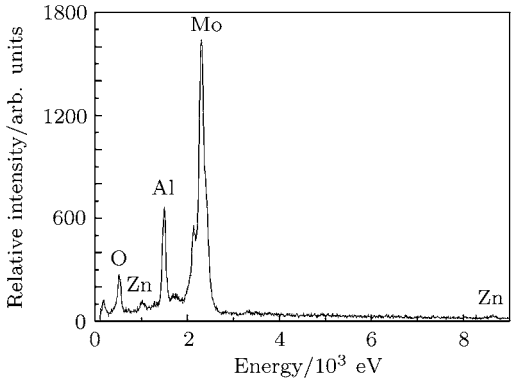


Fig. 1. Energy dispersive spectrum of ZnO film sample.

The surface morphologies, microstructures and surface resistances of NZFs were characterized by a field emission scanning electron microscope (FESEM), the X-ray diffraction (XRD) spectrum, the energy dispersive spectrum (EDS) and a surface resistance meter. The XRD spectrum of the NZFs contains the peaks of the ceramic substrates (Al_2O_3) as well as the peaks of Mo layers, but there is no ZnO layer peak, so we tend to think that the main reason is that the ZnO layer is too thin and the signal is too weak. Figure 1 shows the EDS of the sample film, in addition to the characteristic peaks of Al, Mo and O, the peaks of the Zn appear. This indirectly proves that our samples contain ZnO components.

We find that after hydrogen plasma treatment, both the surface microstructure and the surface resistance of the ZnO films significantly change. Figures 2(a) and 2(b) respectively show typical FESEM images taken from un-treated NZFs and hydrogen plasma treated NZFs. Their corresponding magnifications are also shown in Figs. 2(c) and 2(d), and Figs. 2(e) and 2(f), respectively. It is found that the surface morphologies of the NZFs treated by the hydrogen plasma etching have changed remarkably.

As can be seen from Figs. 2(a), 2(c), and 2(e), the honeycomb-shape NZFs have grown randomly over the entire surface of the Mo layer, and are composed mainly of granulated nano-ZnO grains, (50 nm–100 nm). However, for the hydrogen plasma treated sample, vertically standing and mutually intersecting ZnO nanosheet films (VIZNSFs) are formed regularly

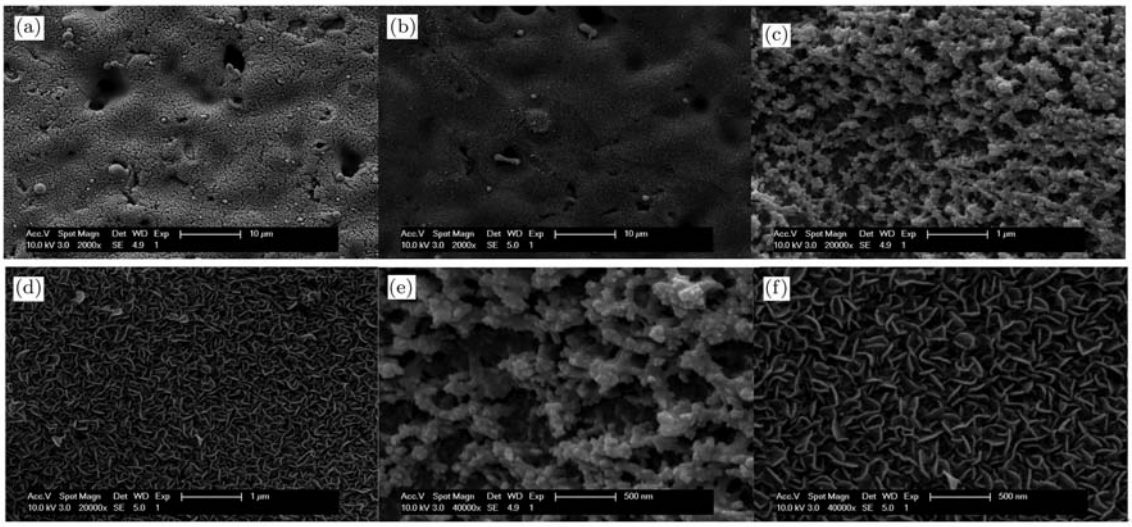


Fig. 2. Field emission scanning electron microscope images of the ZnO films deposited on Mo layer, where panel (a) is for un-treated sample, panel (b) for hydrogen plasma treated sample, and panels (c) and (d), and panels (e) and (f) are for the magnifications of panels (a) and (b), respectively.

on the Mo layer, as shown in Figs. 2(b), 2(d), and 2(f), respectively, the thickness of ZnO nanosheets are typically 12 nm–20 nm. For the hydrogen plasma treated NZFs, the surface resistance decreases to 100 kΩ per square from 10 MΩ per square (for untreated NZFs). Obviously, NZF surface structure and surface resistance changes are attributed to the hydrogen plasma treatment.

2.2. Field electron emission result and discussion

Finally, a functional field emission device was made by using NZFs film/Mo film/Al_2O_3 ceramic as a cold cathode, glass/indium-tin oxide (ITO) film with fluorescent coat as anode, and keeping cathode and anode apart by a 220-μm insulating sheet of mica film. This NZF field emitter was placed in a vacuum system with a Hyvac pump operating at a base pressure of about 5.0×10^{-5} Pa.

Typical curves of J–E were depicted in Fig. 3(a). In this study, FE current density was roughly obtained only by dividing the measured FE current by the area of sample (4.0 cm^2), the threshold E (E_{th}) was defined as E at which $J = 10$ μA/cm^2. For the un-treated sample, E_{th} was found to be 1.1 V/μm and a current density of 39 μA/cm^2 was obtained at an electric field of 4.27 V/μm. For the hydrogen plasma treated sample, the threshold field increases to 1.2 V/μm, but as shown in Fig. 3(a), the observed J rapidly increases with E increasing and exceeds 0.11 mA/cm^2 at $E = 2.47$ V/μm. Figure 3(a) shows a series of J–E data including the 1st, 3rd and 5th measurements (for hydrogen plasma treated sample), indicating that the present H-treated sample yields a reasonable reproducibility of the J–E characteristics only after several sufficiently high E values. Figure 3(b) shows the Fowler–Nordheim (FN) plots, where obviously the J–E data of the un-treated sample do not follow the original FN relation since they are not well represented in the FN plot by a negative slope straight line, which does not show the traditional cold cathode emission and does not correspond to a classical electron tunneling mechanism. For the hydrogen plasma-treated sample, the nonlinear characteristic of the FN plot does not occur ($E > 0.86$ V/μm), the FN plot is a negative slope straight line corresponding to classical electron tunneling mechanism.

These experimental results can be explained as follows. There are a lot of high-energy hydrogen ions and high-energy electrons in the hydrogen plasma, they play an important role in transferring the microstructure of the ZnO films. In addition, hydrogen ions and electrons will inevitably enter into the ZnO film, which will form some special surface states and lead to the ZnO thin film changes in structure and surface resistance. Furthermore, these electrons, which are injected into the NZF, enter into the conduction band of nano-ZnO material more easily, thereby directly leading to the decrease of surface resistance and the improvement of field emission characteristics of NZF.

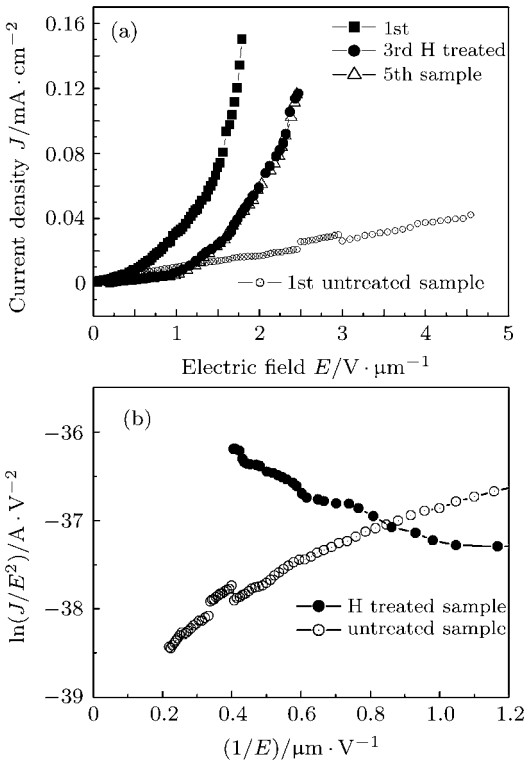


Fig. 3. (a) Plots for emission current density (J) versus electric field (E) of the NSF sample, and (b) plots for Fowler–Nordheim (FN) from NSFs.

3. Conclusions

VIZNSFs are successfully deposited on Mo layers using the catalyst-free electron beam deposition technique and the hydrogen plasma treatment technique. A lowest turn-on field of 1.2 V/μm, high average emission current density of 0.11 mA/cm^2 at a macroscopic electric field of 2.47 V/μm are obtained from the VIZNSF. In addition, for the hydrogen plasma-treated sample, the field emission current density increases more than four times at an electric field of 2.47 V/μm. Its surface resistance, which is measured by a square resistance tester (model KDY-1), can be reduced to 100 kΩ per square from 10 MΩ per square.

The macroscopic FE areas of the measured samples are 4.0 cm^2. The higher emission current density is considered to be due to the unique geometry structure and lower surface resistance of the VIZNSF.

References

[1] Cong G W, Wei H Y, Zhang P F, Peng W Q, Wu J J, Liu X L, Jiao C M, Hu W G, Zhu Q S and Wang Z G 2005 *Appl. Phys. Lett.* **87** 231903

[2] Wang X D, Summers C J and Wang Z L 2004 *Nano. Lett.* **4** 423

[3] Jie J S, Wang G Z, Chen Y M, Han X H, Wang Q T, Xu B and Hou J G 2005 *Appl. Phys. Lett.* **86** 031909

[4] Kong Y C, Yu D P, Zhang B, Fang W and Feng S Q 2001 *Appl. Phys. Lett.* **78** 407

[5] Xu D H, Deng Z B, Xu Y, Xiao J, Liang C J, Pei Z L and Sun C 2005 *Phys. Lett.* A **346** 148

[6] Lee C J, Lee T J, Lyu S C, Zhang Y, Ruh H and Lee H J 2002 *Appl. Phys. Lett.* **81** 3648

[7] Xu C X and Sun X W 2003 *Appl. Phys. Lett.* **83** 3806

[8] Chen Z H, Tang Y B, Liu Y, Yuan G D, Zhang W F, Zapien J A, Bello I, Zhang W J, Lee C S and Lee S T 2009 *J. Appl. Phys.* **106** 064303

[9] Maiti U N, Chattopadhyay K K, Karan S and Mallik B 2010 *Scripta Materialia* **62** 305

[10] George A, Kumari P, Soin N, Roy S S and Mc Laughlin J A 2010 *Mater. Chem. Phys.* **123** 634

[11] Wang A H, Zhong Z G, Cheng L, Lü L X, Wang X C and Zhang B L 2011 *Physica* B **406** 1049

[12] Farid J S, Dilip S J and Mahendra A M 2010 *Thin Solid Films* **519** 184

[13] Farid J S, Dilip S J, Mahendra A M, Jai S and Srivasatva O N 2010 *Mater. Chem. Phys.* **120** 691

[14] Wang X D, Song J H, Liu J and Wang Z L 2007 *Science* **316** 102

[15] Yu W D, Li X M, Gao X D, Qiu P S, Cheng W X and Ding A L 2004 *Appl. Phys.* A: *Mater. Sci. Process.* **79** 453

[16] Hong J and Kae D 2001 *IEEE Transactions on Consumer Electronics* **47** 802

[17] Lan W, Tang G M, Cao W L, Liu X Q and Wang Y Y 2009 *Acta Phys. Sin.* **58** 8501 (in Chinese)

[18] Zhu Y B, Hu W, Na J, He F, Zhou Y L and Chen C 2011 *Chin. Phys.* B **20** 047301

[19] Zang H, Wang Z G, Pang L L, Wei K F, Yao C F, Shen T L, Sun J R, Ma Y Z, Gou J, Sheng Y B and Zhu Y B 2010 *Acta Phys. Sin.* **59** 4831 (in Chinese)